Responsive brushes and gels as components of soft nanotechnology

Article *in* Faraday Discussions · February 2005

DOI: 10.1039/B405700G · Source: PubMed

14 authors, including:

Anthony Ryan
The University of Sheffield
387 PUBLICATIONS **23,764** CITATIONS
SEE PROFILE

Colin J. Crook
The University of Sheffield
16 PUBLICATIONS **693** CITATIONS
SEE PROFILE

Paul D Topham
Aston University
161 PUBLICATIONS **3,288** CITATIONS
SEE PROFILE

Andrew John Parnell
The University of Sheffield
130 PUBLICATIONS **3,041** CITATIONS
SEE PROFILE

Responsive brushes and gels as components of soft nanotechnology

A. J. Ryan,[a] C. J. Crook,[a] J. R. Howse,[a] P. Topham,[a] R. A. L. Jones,[b] M. Geoghegan,[b] A. J. Parnell,[b] L. Ruiz-Pérez,[b] S. J. Martin,[b] A. Cadby,[b] A. Menelle,[c] J. R. P. Webster,[d] A. J. Gleeson[e] and W. Bras[f]

[a] *Department of Chemistry, University of Sheffield, Sheffield, UK*
[b] *Department of Physics and Astronomy, University of Sheffield, Sheffield, UK*
[c] *Laboratoire Léon Brillouin, CEA-Saclay, F-91191, Gif-sur-Yvette Cédex, France*
[d] *ISIS Facility, Rutherford Appleton Laboratory, Chilton, Didcot, Oxfordshire, UK, OX11 OQX*
[e] *CCLRC Daresbury Laboratory, Warrington, UK, WA4 4AD*
[f] *DUBBLE CRG, ESRF, 6 rue Jules Horowitz, BP 220, F-38043, Grenoble Cédex 9, France*

Received 15th April 2004, Accepted 10th May 2004
First published as an Advance Article on the web 14th September 2004

Progress in the development of generic molecular devices based on responsive polymers is discussed. Characterisation of specially synthesised polyelectrolyte gels, ''grafted from'' brushes and triblock copolymers is reported. A Landolt pH-oscillator, based on bromate/sulfite/ferrocyanide, with a room temperature period of 20 min and a range of $3.1 < \mathrm{pH} < 7.0$, has been used to drive periodic oscillations in volume in a pH responsive hydrogel. The gel is coupled to the reaction and changes volume by a factor of at least 6. A continuously stirred, constant volume, tank reactor was set-up on an optical microscope and the reaction pH and gel size monitored. The cyclic force generation of this system has been measured directly in a modified JKR experiment. The responsive nature of polyelectrolyte brushes, grown by surface initiated ATRP, have been characterised by scanning force microscopy, neutron reflectometry and single molecule force measurements. Triblock copolymers, based on hydrophobic end-blocks and either polyacid or polybase mid-block, have been used to produce polymer gels where the deformation of the molecules can be followed directly by SAXS and a correlation between molecular shape change and macroscopic deformation has been established. The three systems studied allow both the macroscopic and a molecular response to be investigated independently for the crosslinked gels and the brushes. The triblock copolymers demonstrate that the individual response of the polyelectrolyte molecules scale-up to give the macroscopic response of the system in an oscillating chemical reaction.

Introduction

The ability of individual polymer molecules to respond to changes in temperature and chemical environment with drastic changes in size and conformation has been appreciated for many years.

The volume transition of responsive gels represents a direct, macroscopic manifestation of the conformational response of the individual molecules making up the gel.[1] Responsive gels have been enthusiastically greeted as candidates for a new generation of intelligent materials with sensor, processor and actuator functions. A wide variety of different stimuli-responsive gels have been developed for specific applications such as drug release and actuators for artificial muscle.[2] However, macroscopic applications of stimulus responsive gels have not developed as fast as was initially anticipated. Part of the reason for this is the fact that diffusion limits the rate at which the gel can respond to changes in environment. Sometimes this simply leads to impractically long response times, but it can also give rise to internal stresses within the gel, as one part attempts to shrink while nearby regions stay swollen, which ultimately can lead to cracking and total mechanical failure.

The scaling of diffusion with size suggests that these undesirable features of gel response will become less severe with decreasing size. Examples of microscopic applications of responsive gels include "flow-sorter" valves for fluidic systems,[3] where the volume transition of the gels open and close 200 μm channels. The ultimate in miniaturisation occurs in polymer brushes, where a single layer of polymer molecules is end-grafted to a solid substrate. For polymer brushes, changes in the environment translate directly into changes in the thickness of the polymer layer.[4] One way in which these thickness changes have been exploited is to line nanoscale pores in a membrane with a pH responsive brush, resulting in a membrane whose permeability alters with the acidity of the environment.[5] Another recent application exploits the fact that a collapsed polymer brush offers a much more favourable surface for protein adsorption than an expanded one to create a programmable surface to hold and release proteins on demand.[6]

One feature of the collapse transition in responsive polymers, whether in the form of a macroscopic gel or as a polymer brush, is that it represents a direct coupling between the chemical environment and a mechanical response. A device which converts chemical energy directly into mechanical energy at a molecular level is known as a molecular motor. Molecular motors are ubiquitous in nature, but synthetic analogues are almost unknown. Although the variety of biological molecular motors is huge, in many cases the basic mode of operation is the same-the "power stroke" of the motor is produced by a *molecular conformational change* induced by a *cyclic chemical reaction*.[7] This mechanism is profoundly different from any used in a macroscopic motor, because it depends fundamentally on the random Brownian motion of the components of the motor. Not only is the "piston" of a molecular motor not stiff as we would try to achieve in a macroscopic engine, its very operation depends on its flexibility, because it is the random Brownian motions within the motor macromolecule that lead to the conformational changes that drive the motor.

At this fundamental level, nanodevices that exploit chain collapse have a broad analogy with the natural nanodevices of cell biology. They exploit the different physics that pertains at the nanoscale in aqueous solution. In this environment, the presence of large dissipation and the dominance of Brownian motion and strong surface forces means that the engineering principles we employ to make nanoscale devices should be very different from the world of engineering at the macroscale. In our experimental program, we attempt to use chain collapse as the basis of nanodevices, that although crude, employ some of the same design principles as cell biology. We hope that these efforts will provide the beginnings of what we might call *biomimetic nanotechnology* or *soft nanotechnology*.

An obvious target for such a program is the development of an autonomously cycling molecular motor, in which cycles of mechanical work are continuously repeated for as long as an input of chemical fuel is maintained. At the macroscopic level, a prototype of such a free-running chemical motor is provided in pioneering studies carried out by Yoshida and coworkers.[8–12] They have coupled the collapse phenomenon in macroscopic responsive gels with oscillating chemical reactions (such as the Belousov–Zhabotinsky, BZ, reaction) to create conditions where "pseudo" non-equilibrium systems which maintain rhythmical oscillations can be demonstrated, in both quiescent[9] and continuously stirred[10] reactors. The ruthenium complex of the BZ reaction was introduced as a functional group into poly(*N*-isopropyl acrylamide) (PNIPAM), which is a temperature-sensitive polymer.[8] The ruthenium group plays its part in the BZ reaction, and the oxidation state of the catalyst changes the collapse temperature of the gel.[10] The result is, at intermediate temperature, a gel whose shape oscillated (by a factor of 2 in volume) in a BZ reaction, providing an elegant

demonstration of oscillation in a polymer gel. This system, however, is limited by the concentration of the catalyst which has to remain relatively small.[12]

In our program, we concentrate on weak polyacids and polybases, which respond to changes in pH. At the macroscopic level, these systems, when coupled with a chemical reaction that cause spontaneous pH oscillations, allow us to make a free-running chemical motor. To miniaturise this to the single molecule level, we need to develop chemical routes to create well characterised polyelectrolyte brushes. We have characterised the response of these brushes to changes in pH by using scanning force microscopy (SFM) and neutron reflectometry. The latter technique, in particular, allows us to follow the collapse transition in some detail. Having confirmed that our polyelectrolyte brushes do indeed exhibit a substantial conformational change in response to changes in pH, our next step was to characterise the way the mechanical properties of a single chain change in response to pH changes. This we have achieved by carrying out single molecule force measurements in a molecular force probe, an atomic force microscope optimised for carrying out force measurements. These results give us the information we need to analyse a motor cycle in our target single molecule synthetic motor. In addition, we are able to quantify the degree to which our polyelectrolyte brushes act as surfaces with switchable adhesion. Finally, we explicitly link the macroscopic behaviour by studying the response of triblock copolymers to pH oscillations. The active chains are the mid-blocks and are effectively crosslinked by the domains of the hydrophobic end block. The expansion and contraction of the grafted polyelectrolyte chains causes the distance between hydrophobic domains to change, this separation can be monitored by SAXS and the molecular and macroscopic effects correlated.

Experimental

Synthesis section

Experimental studies are reported on four related polymer systems. Crosslinked polyacid gels have been described previously[13,14] and the results are included here for completeness. Triblock copolymers were synthesized by living anionic polymerization. A precursor polymer was made with a mid-block of poly(*tert*-butyl methacrylate) and end blocks of polymethylmethacrylate (PMMA). The tertiary butyl ester was subsequently hydrolysed to give the parent polymethacrylic acid (PMAA). Polymer brushes, comprising polyacid (PMAA) and polybase chains, poly((diethylamino)ethyl methacrylate) (PDEAMA), were grown from functionalized surfaces by atom transfer radical polymerization (ATRP). The polyacid was formed by hydrolyzing a poly(*tert*-butyl methacrylate) brush whereas the polybase brush was grown directly.

Polyacid brushes

The substrates used were silicon wafers (Mitsubishi Research and Crystran Ltd.) polished to the (100) face and having a native oxide thickness of 15 Å. The silicon surface was rendered hydrophilic by first cleaning in an oxygen plasma for 10 min followed by the RCA method stage 1[15] (pure water, ammonia (37%) and hydrogen peroxide (20% v/v) with a volume ratio of 5 : 1 : 1, respectively at 80 °C for 10 min). The sample was then washed repeatedly with clean water. The cleaned silicon was dried under a nitrogen atmosphere for several minutes to remove all traces of water. The sample was then transferred to a refluxing environment of 5% (v/v) 3-aminopropyltriethoxysilane in toluene. The sample was held in place for 16 h using a specially designed PTFE holder at a height just above the condensing region. Once removed the sample was placed in a reaction vessel containing a solution of 2-bromo-2-methylpropionic acid (33.4 mg, 0.20 mmol) and *p*-(dimethyl amino) pyridine (6 mg, 0.05 mmol) in 10 ml of dry dichloromethane.[16] The solution was cooled to 0 °C before adding dicyclohexylcarbodiimide (51.6 mg, 0.25 mmol). The wafers were left at room temperature overnight before being washed with toluene and acetone. Before being transferred to the polymerisation medium the wafers were dried with nitrogen.

The chemicals employed in the synthesis were purified as follows: *tert*-butyl methacrylate (tBuMA)(Aldrich, 98%) was stirred over CaH_2 overnight before being distilled under reduced pressure. *N*,*N*,*N*′,*N*′,*N*″-pentamethyldiethylene-triamine (PMDETA) (Aldrich 99%) was used as received. Cu(I)Br (Aldrich, 98%) was stirred with glacial acetic acid overnight, before being filtered

and thoroughly washed with ethanol and acetone, and then dried under vacuum. Benzonitrile (Aldrich, 98%) was used as supplied.

Methyl-2-bromoprionate (0.103 ml, 9.25×10^{-4} mol), Cu(I)Br (133 mg, 0.925 mmol) and 1 ml of benzonitrile, were introduced to a reaction tube. The mixture was stirred vigorously under an inert atmosphere for 20 min before the addition of PMDETA (0.579 ml, 2.78×10^{-3} mol), resulting in the development of an intense green colour. After another 20 min, tBuMA (15 ml, 9.2×10^{-2} mol) was added and stirred until homogeneous. An initiator-coated silicon wafer, held in a wire cradle was then lowered into the mixture, and the temperature raised to 100 °C. The polymerisation mixture rapidly increased in viscosity and, after a period of an hour, the silicon wafer was removed from the vessel and was washed clean in tetrahydrofuran (THF). The free polymer was dissolved in THF and recovered by precipitation in methanol/water (95/5) mixture. The polymer was then filtered and cleaned by further dissolving/precipitating cycles. Following polymerisation the brushes were hydrolysed to remove the *t*-butyl group by refluxing in a solution *p*-toluene sulfonic acid in 1,4-dioxane. Sacrificial free polymer was used in order to reach ideal concentrations, *i.e.* 20% polymer in solution and 5% acid with respect to polymer. The brushes were then removed and placed in a water/methanol mixture followed by several wash steps with deionised water.

Polybase brushes

The substrates were the same as those used for polyacid brush synthesis, $30 \times 30 \times 10$ mm pieces of silicon polished to the (100) face and having a native oxide thickness of 15 Å. These samples were required for neutron reflectivity experiments and so were prepared on large silicon blocks to provide a large surface area and suitable thickness for the reflection geometry. The initiator surface was generated by a 2-step process and differs slightly from that used in the generation of PMAA brushes as described above. Here we attached the initiator to the surface in a single step transfer using (11-(2-bromo-2-methyl)propionyloxy)undecyl trichlorosilane as described by Beers *et al.*[17] and shown in Fig. 1. The silicon surface was rendered hydrophilic as described above and dried in a vacuum oven at 120 °C for 30 min before placing in a PTFE beaker with a tight fitting lid containing 20 ml of a 1.5 μl ml^{-1} solution of trichlorosilane initiator in dry toluene. After the required period the silicon block was removed and subjected to washings with toluene (×2), acetone, and ethanol before finally dried under nitrogen. The blocks were stored under vacuum until required for the brush synthesis.

(Diethylamino)ethyl methacrylate (DEAMA) (Aldrich, 99%) was stirred over calcium hydride overnight before being distilled under high vacuum at 70 °C. PMDETA (Aldrich 99%) was used as received. Cu(I)Br (Aldrich, 98%) was stirred with glacial acetic acid overnight, before being filtered and thoroughly washed with ethanol and acetone, and then dried under vacuum. THF was distilled over sodium/potassium benzophenone and stored under vacuum before use.

Copper (I) bromide (163 mg, 1.14 mmol) and PMDETA (270 μl, 1.29 mmol) were added to 15 ml of stirred THF. The reagents were purged with nitrogen and thoroughly mixed, to which the DEAMA monomer (25 ml, 124 mmol) was subsequently introduced. After 20 min of further stirring, whilst maintaining the flow of nitrogen, the suspended initiators were lowered into the bright blue solution at 75 °C. After 17 h, the silicon-based polymer brushes were withdrawn from the solution (now dark green) and purified using a THF soxhlet reflux system for 24 h. A reference wafer with a saturated initiator surface of dimensions 10 mm × 10 mm × 0.625 mm was also used for each polymerisation bath to assess the consistency of polymer chain growth. With the absence of any direct means of measuring the polymer chain molecular weight the use of a reference wafer allows for some assessment of the molecular weight of the polymer chains on the dilute brush under study.

Block copolymers

Methyl methacrylate (Aldrich, 98%) and *tert*-butyl methacrylate (Aldrich, 98%) were stirred overnight with CaH_2 and then distilled under reduced pressure prior to use. THF was dried using sodium/potassium alloy, and then stored over sodium benzophenone, using the deep purple colour as an indicator of dryness. Double diphenyl ethylene (DDPE) was synthesised by the method previously reported.[18]

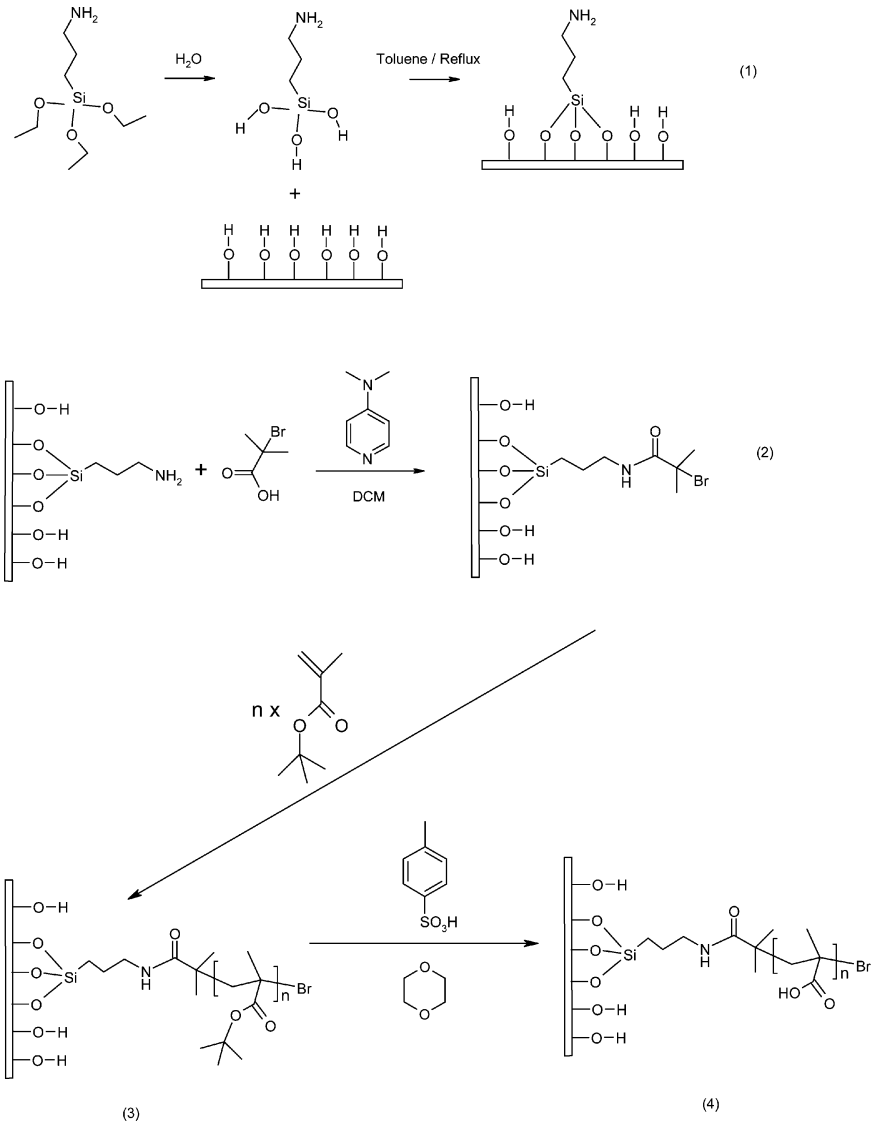

Scheme 1 Formation of polymethacrylic acid brushes.

All procedures were carried out under high vacuum conditions. The required amount of DDPE was weighed into a vessel equipped with a Young's tap, and then placed onto a high vacuum line and evacuated overnight to ensure dryness. Then approximately 10 ml of dry THF were distilled

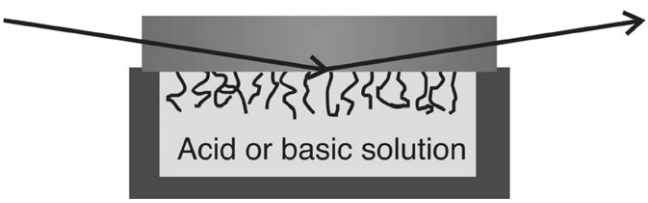

Fig. 1 A schematic representation of the neutron reflectivity geometry.

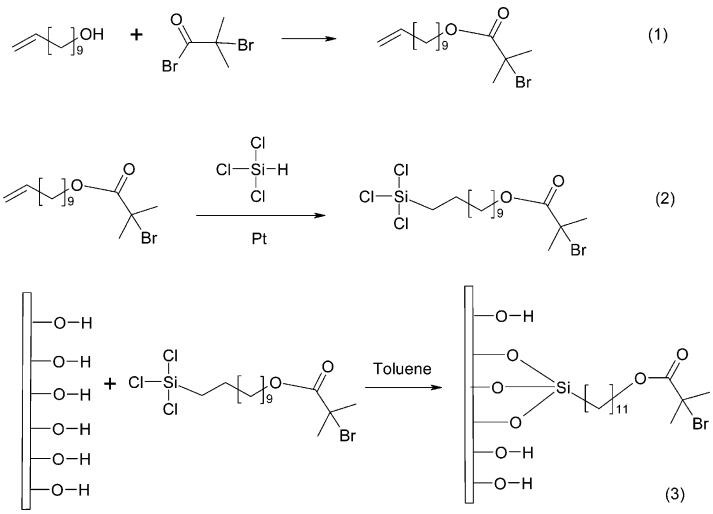

Scheme 2 Formation of the initiator surface for polybase brushes.

over. Into two similar vessels were distilled methyl methacrylate (MMA) and tBuMA. The three vessels and the required ampoule of *sec*-butyl lithium were then affixed to a four-armed vessel with a tap, containing a stainless steel breaker. The vessel was charged with LiCl (a five time molar excess with respect to *sec*-butyl lithium) and then evacuated. It was heated in an oil bath to 130 °C, and the combination of heat and vacuum used to dry the LiCl overnight. 100 ml of dry THF were then distilled into the vessel. The polymerisation was started by opening the initiator ampoule using the metal breaker, and allowing the contents into the vessel. The DDPE solution was then added very slowly, resulting in the development of a blood red colour. The reaction mixture was then cooled to −70 °C using a methanol/solid CO_2 bath and the tBuMA added. The red colour disappeared, and the solution became increasingly viscous over the course of approximately one hour. After three hours, the polymerisation was judged to have finished, and the second monomer (MMA) was added with vigorous mixing. After a further three hours the vessel was frozen and methanol distilled in to terminate the reaction.

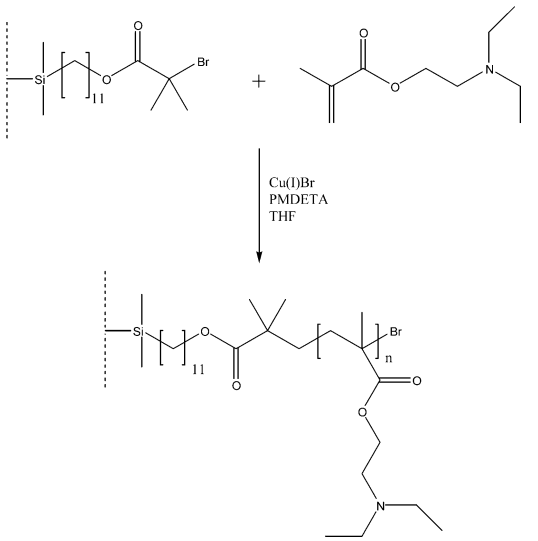

Scheme 3 Preparation of polybase brushes.

Table 1 Molecular characterisation

Code	M_n/kg mol^{-1}	Polydispersity index	Molar ratio$_{PMMA}$
TB56	90	1.24	0.13
TB64	56	1.17	0.13
TB58	155	1.01	0.13

The polymer was purified by precipitation into a methanol/water mixture (90/10 vol). Molecular weights and polydispersities of the polymers were determined using size exclusion chromatography against polystyrene standards, and the molar ratio of the comonomers determined using NMR spectroscopy and are reported in Table 1. The PMMA–tBuMA block copolymers were dissolved in dichloromethane and the tertiary butyl ester hydrolysed by stirring with a 5-fold molar excess of trifluoroacetic acid. The hydrolysed polymer was then precipitated into petroleum ether. NMR analysis showed the hydrolysis to be $\sim$99% complete. The gels were then formulated by dissolving the hydrolysed polymer in 85 : 15 methanol acetone mixture (33% polymer w/v). The thick polymer solution was then sheared between two glass slides to orient the microdomains, and then allowed to dry in a methanol saturated atmosphere for 8 h.

The Landolt oscillating reaction

The reaction mixture used was that reported previously[13,14] and is a development of a range of pH oscillators described by Rabai, Orban and Epstein.[19] Potassium bromate (Aldrich, 99+%), sodium sulfite (Aldrich, 98+%), potassium ferrocyanide (Aldrich, 99+%), and concentrated sulfuric acid (Aldrich) were all used without further purification. Solutions were made using distilled, deionised water and filtered prior to use. The reactions were conducted in an open continuously stirred tank reactor (CSTR), with a peristaltic pump supplying the feed solutions of potassium bromate, sodium sulfite, potassium ferrocyanide and sulfuric acid; and also pumping out bulk solution to keep the volume in the CSTR constant. Measurements of pH were made using a standard gel-filled probe, and the output from the meter monitored by a PC. The optimum flow rate for reliable oscillations was found to be at approximately 0.029 ml s^{-1} with concentrations: $[SO_3^{2-}] = 0.075$ M, $[BrO_3^-] = 0.065$ M, $[Fe(CN)_6^{4-}] = 0.02$ M, $[H_2SO_4] = 0.01$ M.

Scanning force microscopy

Liquid-SFM measurements of the sample were made using a Digital Instruments Multimode Nanoscope IIIa fitted with a J-scan tube (125 μm × 125 μm). Oxide-sharpened silicon nitride (SN-20, Digital Instruments) probes were used. Thin armed 100 μm long cantilevers were driven in the acoustic mode using the standard multimode liquid cell. Resonant frequencies were determined to be 12–13 kHz and Q-enhanced using an Active Resonance controller (Infinitesima). The sample was mounted on a steel puck with a thin film of PTFE attached to the upper surface. The scan tube was protected by placing clingfilm on the head of the tube. Analysis was conducted using Digital Instrument software and the three-dimensional surface plots were generated using WSxM software (Nanotec). Measurements were taken over the same area of the sample with the liquid being introduced through one of the filling holes of the liquid-cell.

Single molecule force experiments

Measurements were made using a molecular force probe (MFP) instrument (Asylum Research Inc.) isolated from vibrations using a Halcyonics active vibration table. The experimental setup uses an open cell arrangement with a wetted SPM tip brought into contact with the wetted sample surface. Commercially available cantilevers (Veeco) were used which had ultra sharp, gold-coated (increased reflectivity) silicon nitride tips calibrated using the thermal method built into the MFP. The tips had a radius of curvature of less than 20 nm (MSCT-AUNM Veeco SPM). A new tip was used after each pH run to reduce tip contamination effects. The brush samples were cleaned with copious amounts of de-ionised water before and after each set of measurements and allowed to equilibrate with the solvent for 5–10 min. This timescale proved adequate as no noticeable change in the force

curve data was observed. The pulling speed of the cantilever tip was kept constant for all data at 800 nm s^{-1} and the tip reversed and approached with no dwell time on the surface.

The MFP measures force as a function of cantilever deflection along the *z*-axis (perpendicular to the sample surface). The observed deflection is made up of the distance between the tip and the sample and the cantilever deflection, therefore to get a true value of the tip–sample distance *D*, and produce meaningful force–distance curves, the cantilever deflection must be subtracted from the *z*-piezo movement to give values for *D*. For a very hard surface, zero separation is defined as the region in the force curve in which the cantilever deflection is coupled 1 : 1 with the sample movement, this appears in the force curve as a straight line of unit slope. A complete force curve includes the measured force profile as the tip probe approaches the sample and is retracted to its initial starting position.

Neutron reflectometry

Neutron reflectometry experiments were performed using the time-of-flight EROS (Orphée reactor of the Laboratoire Léon Brillouin) neutron reflectometer. Although neutron reflectometry is an ideal tool for studying the collapse and swelling of polyelectrolyte brushes, the large sample area necessary for reflectometry experiments has in the past limited studies to polyelectrolytes prepared by the "grafting to" method,[20] although neutron reflectometry has recently been performed on PNIPAM brushes grafted from a silicon surface.[21] Deuterium labelling of the water used to swell the brush provides the necessary contrast with the hydrogenous polybase brush which was grafted from a silicon substrate as described above, and placed in a sample cell, where they could be swollen with a mixture of D_2O and NaOH or HCl as appropriate. The neutron beam passed through the silicon block and reflected from the brush and heavy water interface.

Such a sample geometry is desirable because it provides a highly reflective interface for neutrons, increasing the efficiency by which we can obtain information on the brush profile. In these experiments, we started from a high pH, in which the brush was in a collapsed state, and further experiments were performed with smaller values of pH. After each measurement of the reflectivity for a given swelling (*i.e.* pH value), the silicon wafer with the brush was removed from the sample cell and washed before the next solution was added. In some runs, the brush needed about 30 min to equilibrate (the reflectivity profile changed during the run). The reflectivity data were fitted to model profiles using a Monte Carlo fitting algorithm, as well as a steepest descent fitting routine.

Small angle X-ray scattering

Time resolved SAXS experiments were performed at the Dubble BM26B beam line of the European Synchrotron Radiation Facility (ESRF), Grenoble, France. The ESRF Beam line optics and construction are detailed elsewhere.[22] For comparison, similar SAXS/WAXS experiments were performed on station 16.1 at the Daresbury SRS, UK and the station specifications have been detailed elsewhere previously.[23] The scattering vector axis, *Q*, of the SAXS patterns were calibrated using an oriented sample of rat-tail collagen, while for the spatial calibration of the WAXS patterns use was made of HDPE and NBS (National Bureau of Standards) silicon.

The experiment set-up for studying the triblock gel with SAXS comprised of a Nylon cell with an internal liquid volume of 100 ml. Two hollow nylon bolts with mica windows situated on their ends were screwed in the walls of the cell into the liquid volume to leave a gap of approximately 3 mm. Perpendicular to this were placed two transparent polystyrene windows that allowed illumination and image capture of the gel's macroscopic behaviour. The gel sample was held in place using tweezers. The addition of the solutions of the oscillating chemical reaction was *via* a peristaltic pump and pH was recorded using a combined microelectrode (Mettler Tolledo) connected to a PC situated outside the experimental area.

SAXS images were collected at 60 seconds per frame for a total time of 120 frames (2 hours) whilst situated within the oscillating chemical reaction. The scattering pattern obtained showed a sharp ring indicating a single length-scale within the phase-separated gel. The 2 dimensional data was sector integrated to produce 1D data.

Results

Gels in oscillating reactions

Our general approach uses pH as the stimuli for the responsive polymer and an oscillating stimulus can be given by the the bromate/sulfite/ferrocyanide pH oscillator.[19] The experimental benefits of this system are a reliable oscillation at room temperature, a large pH range (four orders of magnitude in $[H^+]$), and, most importantly an oscillation that remains at the pH extremes for approximately equal times to allow the mass transport (of water and ions) associated with the change in polymer conformation.

The oscillating reaction mechanism of the process is very complicated, consisting of many mechanistic steps, but may be viewed at a simplified level as consisting of two subsystems; the oxidation of sulfite by bromate (1) and the oxidation of ferrocyanide by bromate (2). The first process serves as the proton production mechanism (positive feedback) with an appropriate "induction time", while the second acts as the negative feedback reaction consuming protons.

Careful tuning of both the reactant concentrations and the feed rate to the reactor are required to obtain reliable oscillations and there is obviously an interaction between the feedback process of reaction and the changing degree of dissociation of the polyelectrolyte. The size dependence of the swelling rate of polymer gels is well established,[24] the data in Fig. 2 were obtained for a piece of gel of characteristic dimension 20 μm that could attain equilibrium swelling in a time scale shorter than the period of the oscillating reaction.

Six oscillations are shown here, these were taken from a reaction that had been running for 170 min and continued to run for a further hour. The reliability of the pH change and the response of the gel is readily apparent from the graphs. Whilst the large dimension attained is stable the minimum dimensions seem to be affected by hysteresis, the most likely reason being the difference in the characteristic times for swelling and collapse. In materials which are glassy (or of high polymer concentration) in the collapsed state, collapse takes longer than swelling because the difference in the geometry—a particle that is swelling has a low density corona and a dense core whereas a collapsing particle has a dense shell surrounding a swollen core—which is, therefore, a barrier to solvent diffusion on collapse and mass transport is restricted compared to expansion. In this case, however, the polyelectrolyte is still substantially plasticized by water in the collapsed state and the hydrodynamics are dominated by ion transport and mechanical equilibration, the collapse transition has a characteristic time approximately half that of expansion.[14] The local pH change is

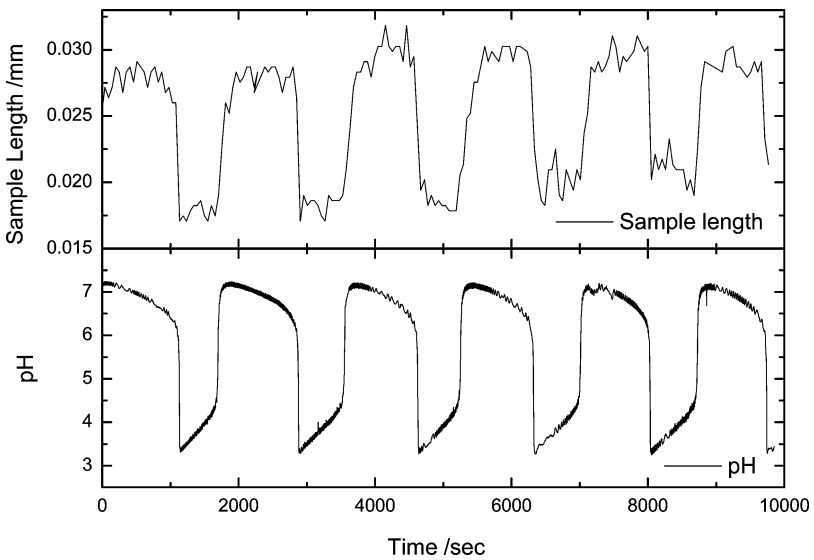

Fig. 2 The variation in pH caused by the oscillating chemical reaction and the associated change in length in the polymer gel.

$$BrO_3^- + 3HSO_3^- + H^+ \longrightarrow Br^- + 3SO_4^{2-} + 4H^+ \quad (1)$$

$$BrO_3^- + 6Fe(CN)_6^{4-} + 6H^+ \longrightarrow Br^- + 6Fe(CN)_6^{3-} + 3H_2O \quad (2)$$

Scheme 4 The fundamental reactions of the Landolt pH oscillator.

effectively instantaneous as protons diffuse rapidly. The sample can collapse completely within one pH cycle but cannot completely expand, this causes a gradual build-up in the ionic strength within the gel as the water diffuses faster than the solvated ions and the hysteresis due to the effective screening of charge.

Measurements were made of the force generated by such a gel in a modified JKR apparatus.[25] The sample is placed on a stage inside a beaker, and then a *Z*-translational stage, controlled by a worm microdrive, is lowered down onto the sample holding it in place. The solutions for the oscillating reaction are then pumped into the beaker with a peristaltic pump until the optimum level is reached, at which point waste is pumped out at an equal rate to maintain a constant volume. The reacting solution is then stirred using a paddle mounted on a 12 V motor, at as slow a rate as possible whilst maintaining good mixing, in order to minimize noise in the readings. The concentrations of the reactants used were the same as used for the swelling experiments. As the gel swells and deswells in the oscillating solution, the translational stage is set in position when the pH is low and the gel contracted, so that it is applying a force in the order of a gram. Changes in this force were then monitored *via* the balance over the course of numerous oscillations (Fig. 3). The pH data are presented as measured. The force data have been smoothed using a fast Fourier transform smoothing function to remove only the stirring noise, as this has a constant and definite frequency.

The oscillation appears to have a longer period, and is less regular, than that seen in Fig. 2. It is not clear whether this is due to a buffering effect of the gel or an effect of the size scale of the reaction vessel. Forces were measured in a reaction taking place in a 100 ml flask whereas the size was measured in a Petri dish with a volume of 25 ml. Although an attempt was made to keep the same residence time in both cases, some kinetic mismatch may occur due to the use of different apparatus volumes, and this could contribute to the change in oscillation period. Over the four hour time period, the force produced can be seen to follow the period of the oscillating reaction indicating that the mass transport through the gel is commensurate with the timescale of the oscillations. The maximum force produced by the gel is 0.012 N. The slight upward drift in the data is due to an increase in mass caused by a small mismatch between the flow rates of the pumps used.

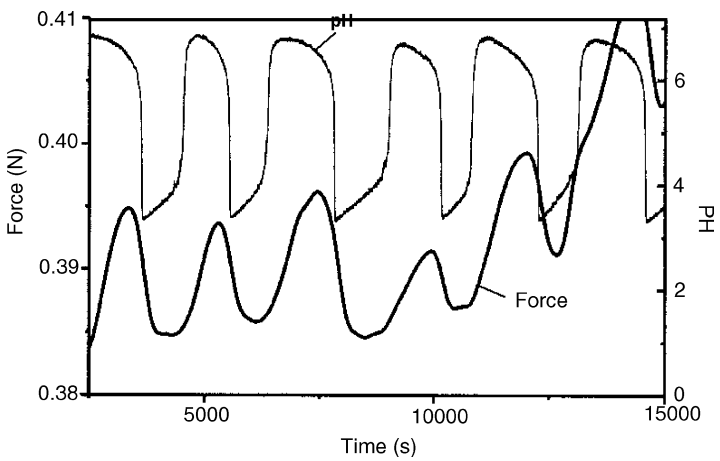

Fig. 3 pH and force *versus* time as the hydrogel responds to the oscillating reaction. Residence time 1000 s, at room temperature. Input concentrations: $[SO_3^{2-}] = 0.075$ M, $[BrO_3^-] = 0.065$ M, $[Fe(CN)_6^{4-}] = 0.02$ M, $[H_2SO_4] = 0.01$ M.

In summary a pH oscillator has been developed to cover the range 3–7 with a time constant of approximately 20 min. The reaction has been coupled with a responsive gel to generate a model system with spatio-temporal oscillations. We have observed macroscopic dimensional changes by optical microscopy and mechanically harnessed the gel to generate force. Of course, the measured force is only a small proportion of the potentially available force, as it is only measured in one dimension and is heavily damped by mass-transport considerations, but it displays that these systems can be used to directly convert chemical potential to mechanical work.

Responsive brushes

The polymer brush used in this study was generated by the ''grafted-from'' approach to generate a brush in the mid- to dense- brush regime. The grafted-from technique requires the anchoring of an initiator to a surface followed by exposure to a polymer generating medium/environment. The ATRP method used for the polymerisation is a living process where a halide is reversibly transferred from the initiator (or growing chain) to a metal halide to leave a radical. This radical will then propagate polymerisation for a short period of time before the halide is transferred back and the growing chain becomes dormant. This results in polymer chains that grow at the same rate coupled with a suppression of side reactions, as the concentration of radicals is always very small at any given time. Initial studies concentrated on the responsive nature of dense PMAA brushes which were grown on Si wafers with the maximum areal density of initiator.

To demonstrate the responsive nature of the dense ''grafted-from'' brushes the brush height was measured as a function of the pH (an ionic strength) of the solvent using SFM. From the images of a PMAA brush in Fig. 4 we can clearly see a marked difference in brush height and brush topography. This we attribute to the brush being in the collapsed (pH 3) and extended (pH 10) state, respectively. The height of the brush was measured by taking a histogram of heights from the upper right-hand corner of both images.

The height is quoted with reference to the bare silicon surface represented by the data at height = 0 nm in Fig. 5. A collapsed height of 86.4 nm with a standard deviation of 16.6 nm was

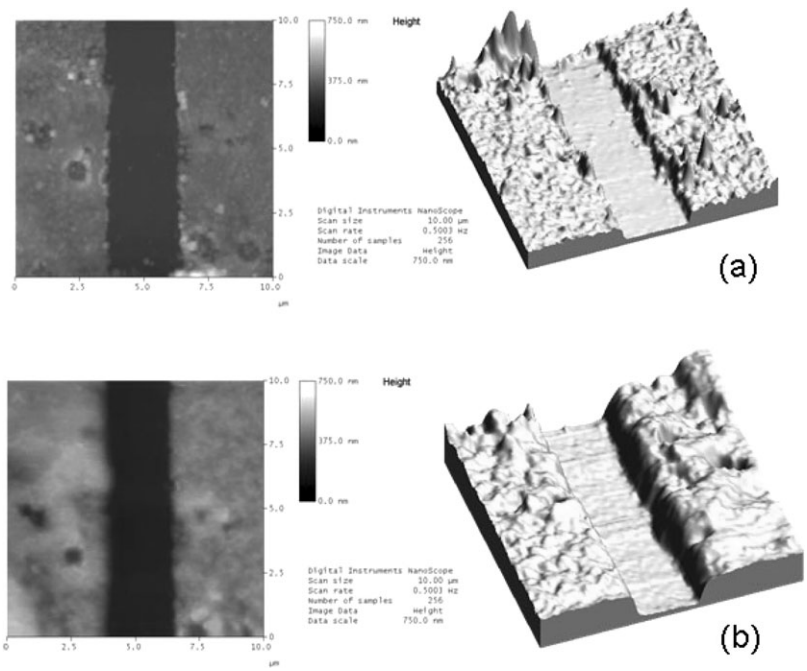

Fig. 4 (a) Collapsed dense polymer brush in dilute H_2SO_4 (pH 3), the dark line in the height image and the trough are a scratch down to the base silicon surface. (b) The same dense polymer brush swollen in dilute NaOH (pH 12).

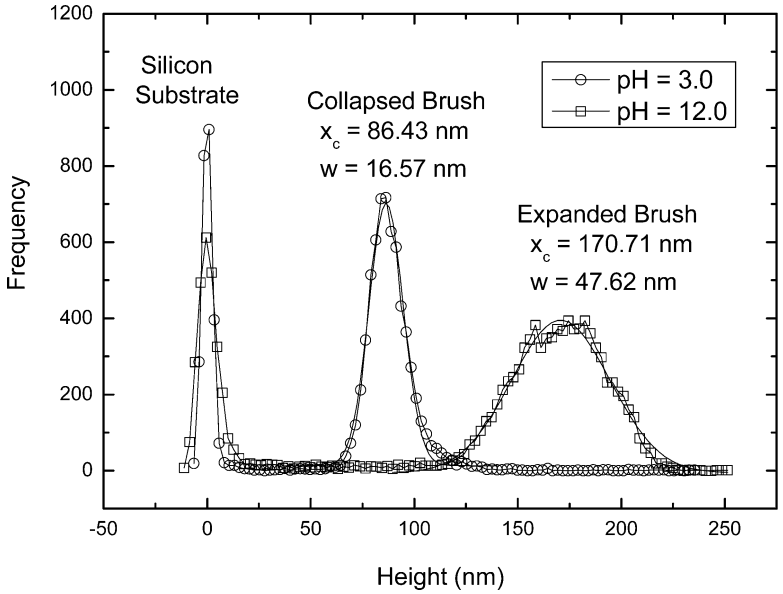

Fig. 5 Histogram of heights determined from the SFM images in Fig. 4. The data are reported as fits to the power spectra of position x_c and distribution w.

measured for acidic conditions. For basic conditions a height of 170.7 nm and a width of 47.6 nm was measured. This represents a swelling by a factor of $\times 1.97$ and is very low compared to that expected from the simple brush collapse model, discussed above. A conservative estimate of the degree of polymerisation of these chains is 300 (taking the dry-brush thickness to be the contour length). This would predict a minimum swelling ratio of at least a factor of 4.6 for a polymer chain.

The low degree of swelling in this thick polymer brush is typical of a polymer brush with chains that were densely packed during synthesis. Because each polymer chain is already stretched (for steric reasons) in the collapsed state the change in brush thickness with pH is rather small. That dense brushes like these had very low degrees of swelling prompted us to develop methods of controlling the surface initiator density as described in the experimental section. The brushes used in the subsequent neutron reflectivity and molecular force experiments had a significantly lower areal chain density to minimise the steric reduction in thickness change.

In Fig. 6 we show sample neutron reflectometry data for a medium areal density PDEAMA brush swollen in D_2O. To fit these data we chose a simple model accounting for single layers of silicon oxide and initiator. The brush profile was fitted to a hyperbolic tangent. In order to limit the number of parameters we used the scattering length densities set from reflectometry experiments performed on the dry brush in air. This enabled us to obtain information about the thickness and scattering length density of the initiator layer, which we could use in the case of the brushes in solution. The dry brush experiments also revealed the thickness of the brush layer in the dry state, which fixes the amount of PDEAMA that we could fit to in the swollen case (*i.e.* the integrated area under the hyperbolic tangent volume fraction profile must be constant and equal to the brush thickness).

Experiments were performed on two brushes with different thicknesses in the dry state (brush thickness increases with both increasing molecular weight and increasing grafting density, which forces the chains to stretch). Typical data and fits for one of the brushes are shown in Fig. 6. There are some systematic deviations between the model curves and the data. This reflects the fact that the fits were highly constrained. Volume fraction-depth profiles for the brush layers are shown in Fig. 7. The trends in the profiles are clear for each brush thickness; the brushes are collapsed for values of pH > 4, but to varying degrees (*i.e.* the width of the hyperbolic tangent profile σ, increases with decreasing pH). For pH < 5, the brush is stretched. The magnitude of the swelling depends on the molecular weight and grafting density of the brushes, as well as the pH. We note that the 130 Å

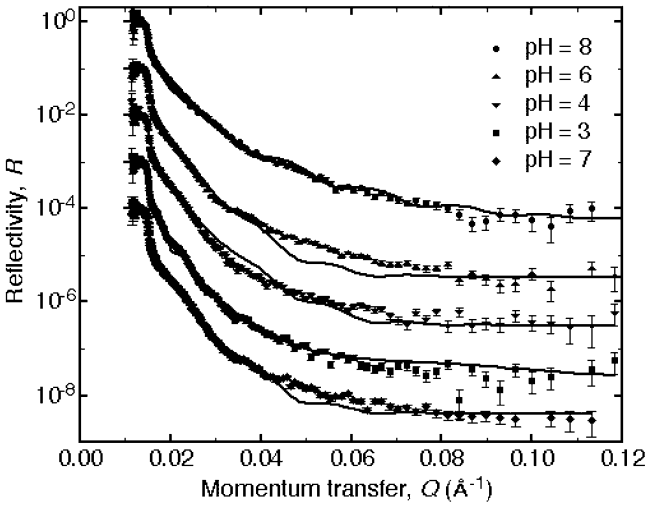

Fig. 6 Neutron reflectivity spectra for a PDEAMA brush in D_2O as a function of pH. For clarity of viewing the data are shifted down vertically by a factor of 10 from each other.

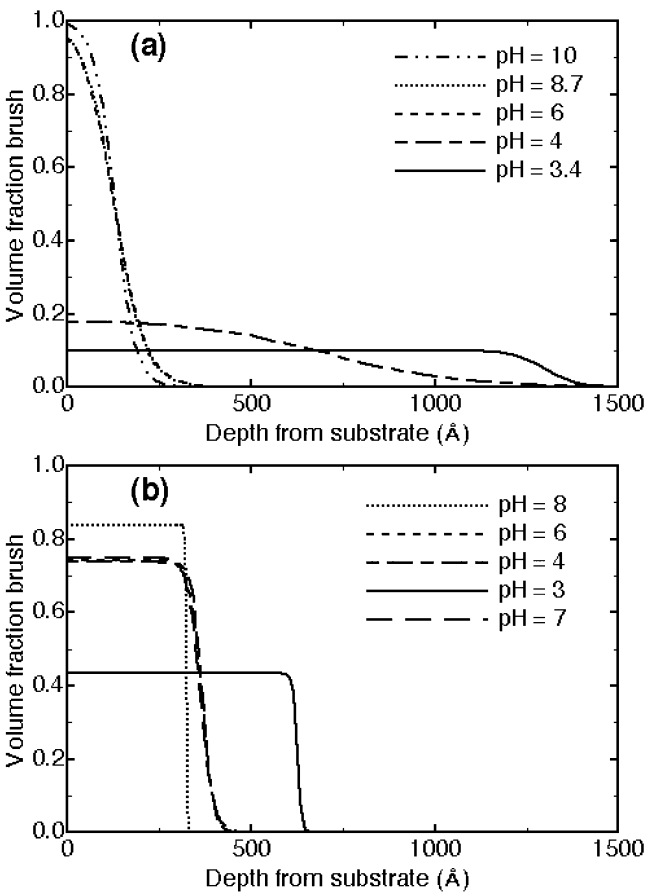

Fig. 7 Volume fraction–depth profiles for a brush of thickness 130 Å (a) and 276 Å (b) in the dry state. The profiles in part (b) correspond to the fits presented in Fig. 6.

brush swollen in pH = 3, swells to a thickness of nearly by 10 times its dry thickness, but that the 276 Å brush hardly swells at all, which suggests an effect of grafting density (a molecular weight effect may also be present, but is expected to play a smaller role here).

The problem inherent in the interpretation of the neutron reflectivity data is that the molecular weight of the chains and their areal density are coupled in a non-linear way in their effects on both the dry brush thickness and the swelling ratio. A dense brush of long chains may swell less than a dilute brush of shorter chains because of steric effects. Whilst we can exercise some degree of control over the initiator we are not currently able to decouple the brush length and the areal density of chains. Furthermore the model that we have used for our profiles is probably rather simplistic. Previous reflectometry experiments have been performed on PNIPAM brushes and the best fits that were achieved have been achieved with a more complex profile than the simple hyperbolic tangent presented here.[21] This will be addressed in future experiments with deuterated polyelectrolyte brushes for increased sensitivity. Another factor, which may be important is that of hysteresis in the swelling. In Fig. 7, we show data for the 276 Å brush swollen in pH = 7. This swelling was performed after swelling in pH = 3. The corresponding fit is consistent with the other data, shown in Fig. 7b, and suggests that such hysteresis may not be a problem, for these samples. However, other (as yet unpublished) data suggest that some hysteresis does indeed exist, and a full study of brush swelling as a function of sample history is lacking. Despite these caveats, neutron reflectometry does show that the PDEAMA brush swells as a function of pH, and that at low pH, the thinner brush indeed swells quite substantially compared to its dry state.

Single molecule force spectroscopy experiments have been previously reported for both natural[26] and synthetic[27] polyelectrolytes. In particular Ortiz and Hadziiannou[28] have studied the force–distance curve of polymethacrylic acid in water, using a *freely jointed chain* (FJC) model to interpret the single molecule behaviour. One of our concerns is that we can assess the "efficiency" of any device we might build in terms of the force developed by a single chain and we have studied the response of PDEAMA in the expanded and contracted states. A Si_3N_4 probe tip was used to pick up the chains *via* non-specific physisorption interactions.

A typical force–distance curve for a collapse (hydrophobic) chain is given in Fig. 8. Far away from the surface the force is zero and there is no interaction between the tip and the sample [region (a) in the figure]. As the cantilever approaches the surface, [region (b)], a nonlinear repulsive force is

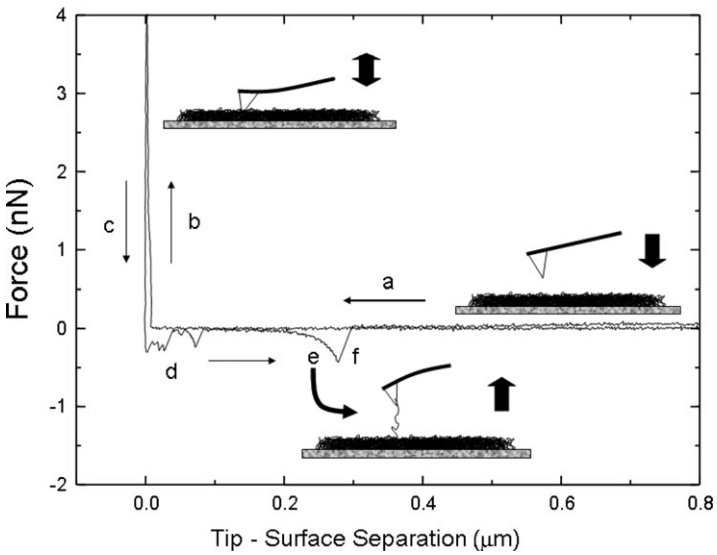

Fig. 8 The anatomy of a typical force–distance curve for a polyacid in the collapsed state capable of adsorption on the SFM tip. (a) Tip approaches surface—no interaction. (b) Tip compression of brush–"hard-sphere" type interaction. (c) Retraction—force acting on the tip decrease as the sample is moved away. (d) Tip pulled down—indicating adhesion/multiple-chain pulling events. (e) Stretching of a single molecule (force curve). (f) Polymer detaches from the tip.

observed corresponding to compression of the brush and this initial reaction can be seen more clearly in Fig. 9a. A detailed discussion of the transition from the squeezing of the brush to the hard-sphere repulsion on contact of the tip and the silicon wafer is beyond the scope of this discussion but the near vertical force–distance curve in region (b) denotes the contact point and compression of the Si wafer. Decompression of the Si is reversible, initially following the same force–distance curve [region (c)] as compression, and there is some hysteresis due to the tip–substrate adhesion but the majority of the attractive force and its instability in region (d) is due to the detachment of many chains. In contrast to previous reports[28] on dilute brushes there is a high likelihood of multiple chain attachment in these dense brushes. As the retraction proceeds a single attractive peak is observed with a nonlinear increase of force with distance [region (e)]. This attractive peak is attributed to the stretching of an individual polymer chain which had become physically adsorbed to the tip and bridges to the surfaces. That this part of the force–distance curve applies to a single chain is borne out by the statistical nature of the data fitted to many such curves. The chain conformation on the surface of the tip; that is a combination of loops, trains and tails; is not known. At sufficiently high extensions the elastic restoring force of the chains becomes greater than the adsorption force tethering the chain segments to the tip and the chain suddenly desorbs and the cantilever returns to its undeflected position corresponding to zero force (f).

Ortiz and Hadziiannou[28] tested a series of models for fitting the force–distance curves to the entropic restoring force due to uncoiling of individual chains. We have fitted our data to the FJC using both the contour length and the statistical segment length of the chain as fitting parameters as the length of chain that is physisorbed to the probe tip is variable so the effective contour length is also a variable even if the chains are all of a unique length. The FJC is expressed as

$$F_{\text{chain}} = {}^{k_{\text{B}}T}/_{aL*(r/L_{\text{c}})}$$

where F_{chain} (nN) is the restoring force produced by the stretched elastic polymer chain, r (nm) is the absorbed chain end to end separation (*i.e.* the tip to surface distance), k_{B} (J K^{-1}) is Boltzmann's constant, T (K) is temperature, a is the statistical segment length (nm) and L^* is the inverse Langevin function. L_{c} (nm) is the fully extended length of the chain (na) where n is the number of chain segments. L_{c} is a fitting parameter since the adsorption length is random even if all the chains have the same number of monomers.

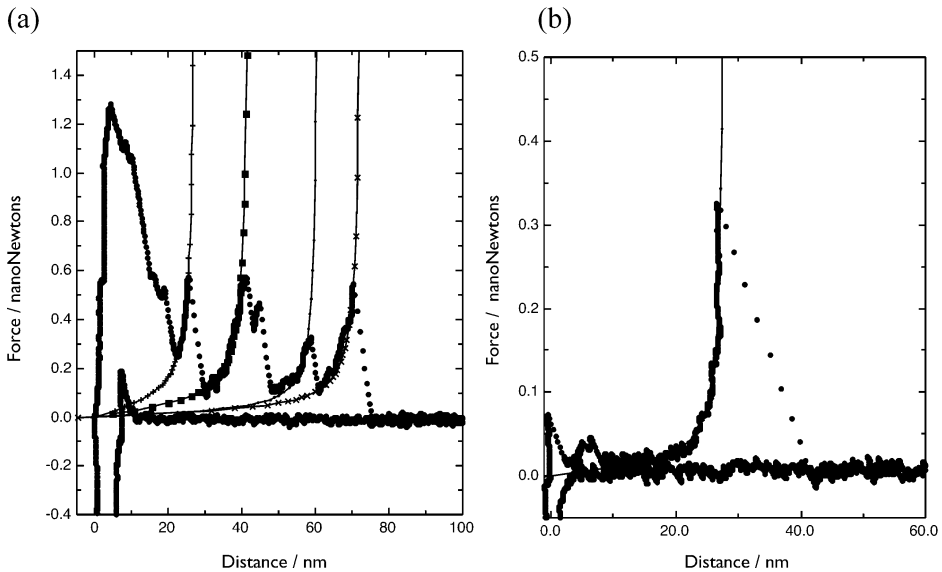

Fig. 9 Force–distance curves for a PDEAMA. The force-axis has been inverted with respect to Fig. 8. The line is a fit of the freely jointed chain model. (a) Pull-off curves at pH 4 with contour length, L_{c}, values of 28, 42, 63 and 73 nm and statistical segments lengths, a, of 0.09, 0.12, 0.18 and 0.23 nm respectively and (b) a pull-off curve in pH 10 buffer with contour length, L_{c}, of 48 nm and statistical segment length of 0.48 nm.

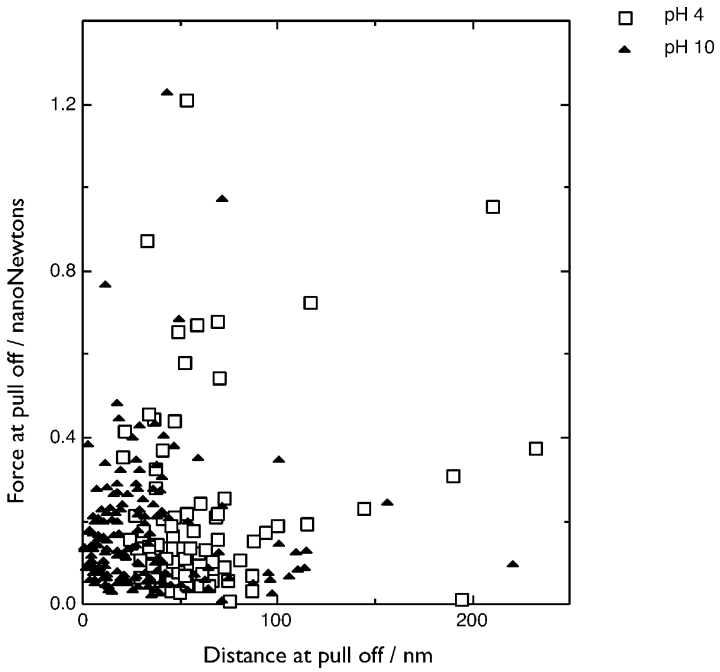

Fig. 10 Pull off values for the force and distance of the collapsed (filled triangles) and swollen (open squares) state of brush sample 12.

The (pH = 4) expanded brush state has a lower statistical segment length corresponding to a more flexible chain, a (pH = 10) = 0.37 nm ± 0.19 nm compared with a (pH = 4) = 0.19 nm ± 0.12 nm. The two sets of curves shown in Fig. 9 are representative of the data. The force–distance curve for the brush immersed in the pH = 4 solution highlights the expanded brush having a large adhesion energy. Near the surface of the brush the chains are in an extended conformation allowing the tip to entangle and attach to more chains than in the collapsed state of the brush. In the collapsed state the chains and the resulting force curves show very little adhesion near the surface, as they are less able to form attachments to the tip due to their collapsed nature.

The data presented in Fig. 10 are the final (pull-off) values of force and distance (L_{PO}) in each force distance curve as the cantilever tip detaches from the surface. The preliminary data for the swollen brush (pH 4) exhibits a larger pull off distance than the contracted (pH 10) force pulls. The average values are 62 ± 41 nm and 32 ± 31 nm respectively.

Further work will concern a more detailed investigation of the brush behaviour in the absence of added salt. Alongside this a variable pH mechanism will be used to look at the switching behaviour of the brush as contact is maintained with the tip.

Block copolymers

To bridge the macroscopic change in dimensions of a polymer gel with the change in conformation of the polyelectrolyte chains we use the glassy hydrophobic domains in a triblock copolymer cubic (spherical) morphology as a molecular calliper. The polymer was designed[29] to have a spherical morphology in the dry state having a volume fraction of ~0.15 hydrophobic PMMA. The hydrophilic polyacid chains would then be able to swell and collapse leaving the hydrophobic domains unaffected, and acting as physical crosslinks. This approach is shown schematically in Fig. 11 where an increase in pH causes ionisation of the PMAA chains and expansion on the nanoscale that propagates through to the unit-cell mesoscale and a serial addition of unit cell volume changes contribute to the macroscopic change in shape of the gel.

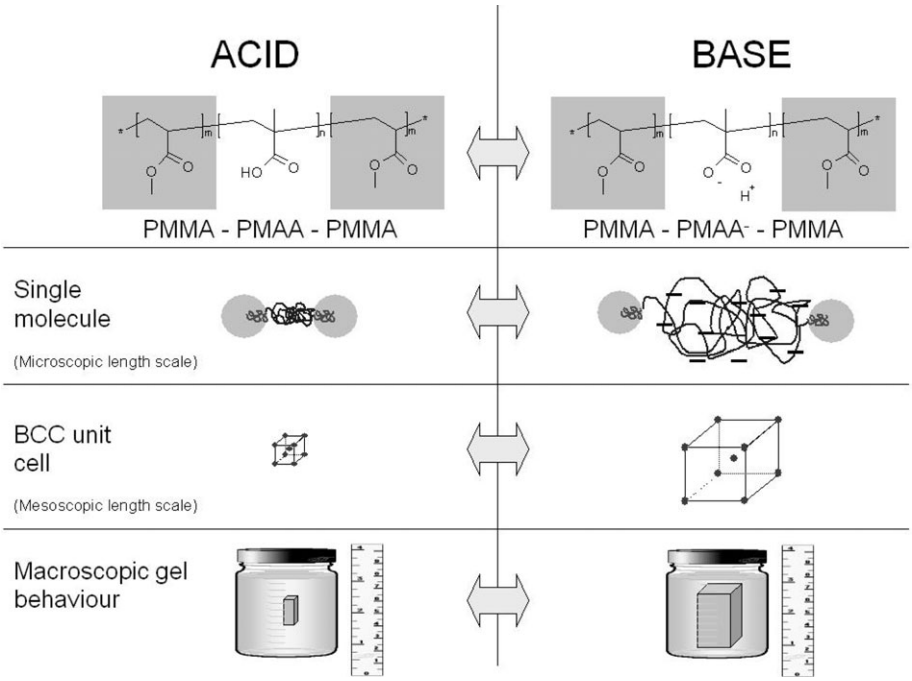

Fig. 11 The cascade of length scales probed in the SAXS study of responsive block copolymer gels.

The triblock copolymer used here was a PMMA–PtBuMA–PMMA (7k–141k–7k) triblock with a polydispersity of 1.01 that was subsequently hydrolysed to yield a mid-block of methacrylic acid and PMMA–PMAA–PMMA (7k–85k–7k). The preparation of a suitable sample for scattering proved difficult as annealing of the melt is not an option due to the glass transition of PMAA being greater than 250 °C. To form a gel approaching equilibrium a solvent casting method was developed using a mixed solvent system—2 miscible solvents that are selective solvents for each block. Acetone and methanol, solvents for PMMA and PMAA respectively, were used at 15 : 85 v/v ratio. (the same ratio as polymer volume fractions.) to make a concentrated solution at 33 wt.% polymer. High concentrations were required to prevent excessive looping of the chains so that the hydrophobes were not both in the same domain—*i.e.* to prevent flower micelle formation and encourage bridging of domains.[30] Acetone has a higher vapour pressure than MeOH and so this evaporates first to generate glassy PMMA domains in a MeOH swollen PMAA matrix. To generate a suitable sample, the concentrated solution was sheared between two glass slides held apart by 300 μm spacers. The slides were then run off each other and placed in a saturated methanol atmosphere for 8 h. To handle the gel, which is glassy in the absence of any solvent, the solvent annealed sample was submerged in water. The polymer gel floated off the glass surface and was cut into a suitable sized piece using a scalpel.

The response of the polymer was first studied in the quiescent state using a trapped gel that was exposed to both acidic and basic solutions. There was an appreciable shift in the peak position, q^*, with pH and the transition time was less than ten minutes. Monitoring the gel-size, by video microscopy, showed the shift in domain spacing to be commensurate with the swelling. The dynamic behaviour of the gels was then studied in the oscillating chemical reaction and the SAXS patterns and images of the gels are shown for both the collapsed and the expanded state in Fig. 12.

As expected the peak in the scattering pattern moved towards lower Q as the pH of the oscillating chemical reaction increased. As the pH suddenly dropped the peak moved towards higher Q. The position of the maximum (q^*) is plotted against the pH of the solution in Fig. 13. From this we see that the gel takes approximately 1 complete cycle of expansion–collapse to establish equilibrium with its surroundings. Also the moment at which the collapse and expansion begins is the point at

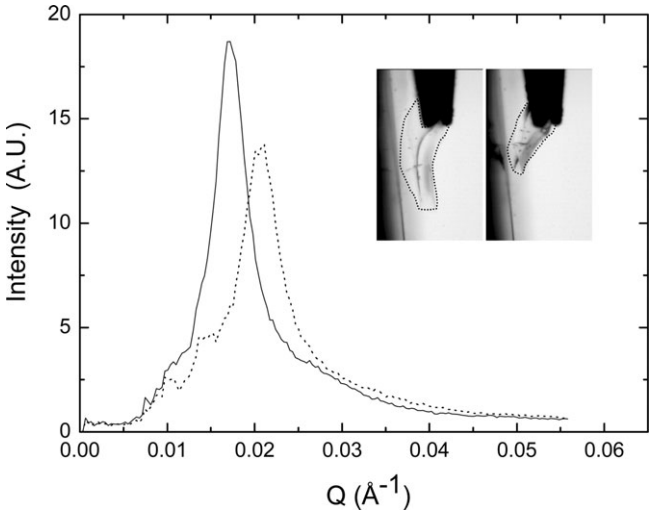

Fig. 12 1D scattering pattern of PMMA–PMAA–PMMA gel in an oscillating chemical reaction at $t = 5$ mins (pH = 6.19) (—) and $t = 15$ mins (pH = 3.66) (···). The macroscopic behavior is shown inset as the expanded and collapsed forms (left, right, respectively). The outline of the gel is indicated to aid the eye.

which the pH is seen to rapidly increase or decrease. The change in length scale shows no signs of damping or hysteresis as the reaction proceeds through several oscillations.

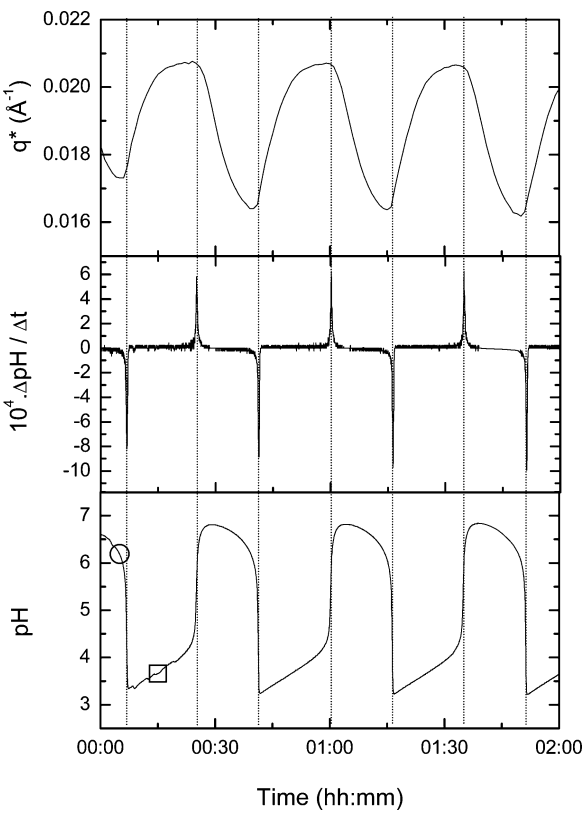

Fig. 13 1D SAXS peak position (q^*) showing the correlation between peak position and change in pH. The data shown in Fig. 12 is marked in the lower graph (○ and □).

Summary

This paper is essentially a report on a work in progress demonstrating that polyelectrolyte chains and oscillating chemical reactions can be coupled to give a system that shows responsiveness that scales additively from the molecular to the macroscopic. As active components we have utilised weak polyacids and polybases, which respond to changes in pH. These have been assembled into covalently linked networks, polymer brushes that are essentially responsive monolayers and triblock copolymers that combine the characteristics of self-assembly and responsiveness. At the macroscopic level, these systems, when coupled with a chemical reaction that cause spontaneous pH oscillations, allow us to make a free-running chemical motor. At the single molecule level, we have characterised the response of these brushes to changes in pH by using scanning force microscopy (SFM) and neutron reflectometry following the collapse transition *in situ*. Furthermore the mechanical properties of a single chain change in response to pH changes have been studied by single molecule force measurements in a molecular force probe, giving us the information to analyse a motor cycle in our target single molecule synthetic motor. In addition, we have quantified the degree to which our polyelectrolyte brushes act as surfaces with switchable adhesion. The macroscopic behaviour of responsive systems is linked to the molecular response by studying the response of triblock copolymers to pH oscillations. The active chains are the mid-blocks and are effectively crosslinked by the domains of the hydrophobic end block which act as molecular callipers. The expansion and contraction of the grafted polyelectrolyte chains causes the distance between hydrophobic domains to change, this separation has been monitored by SAXS allowing the molecular and macroscopic effects correlated for the first time.

There is much current activity in developing systems whose properties are responsive to environmental changes. The laws governing self-assembly processes operate at supra-molecular length scales and are universal, and the specific properties of any objects built this way are defined by their chemical structure. Templating with block copolymers, polypeptides and polyelectrolytes can create structures and build devices for a wide range of applications based on a limited set of physical principles. Polymer science and supra-molecular chemistry have developed to the stage that makes possible the construction of useful devices based on responsiveness and self-assembly. The major theme of this research is the identification of the underpinning technology required for a range of generic passive and active systems and the application of established methods in physical science to the production of *soft-nanotechnology* devices that are inspired by cell-biology. Complex, highly engineered structures are held together by weak bonds (hydrogen bonds, hydrophobic/hydrophilic interactions, screened Coulomb interactions) formed at room temperature and pressure from molecules that have information written into them. The macromolecules are used both as templates and the components of molecular machines. Devices made by these principles are self-assembling and responsive to their environment, they operate in a solvent (preferably water) at a constant, relatively high temperature. Early results from this research might find uses in drug delivery and opto-electronic devices. Longer-term efforts may be directed toward the making of self-propelled vehicles that recognise targets, creating a version of nanotechnology that looks like cell biology.

Acknowledgements

We would like to thank the European Commission for the provision of beamtime on EROS under the ''Large Research Infrastructure'' contract HPRI-CT-2002-00170, the ESRF for beamtime on DUBBLE under the long-term-proposal SC777 and CCLRC for beamtime on 16.1. LRP, CJC, PT, AJP, SJM and AC were supported by EPSRC grants (GR/R77544, GR/R74383, GR/R55573, GR/N02542, GR/M72449) and JRH was supported by ICI PLC.

References

1 M. Shibayama and T. Tanaka, *Adv. Polym. Sci.*, 1993, **109**, 1–62.
2 *Biorelated Polymers and Gels*, ed. T. Okano, Academic Press, San Diego, CA, 1998.
3 D. J. Beebe, J. S. Moore, J. M. Bauer, Q. Yu, R. H. Liu, C. Devadoss and B.-H. Jo, *Nature*, 2000, **404**, 588–590.

4 A. Karim, S. K. Satija, J. F. Douglas, J. F. Ankner and L. J. Fetters, *Phys. Rev. Lett*., 1994, **73**, 3407–3410; M. Sferrazza, R. A. L. Jones and D. G. Bucknall, *Phys. Rev. E*, 1999, **59**, 4434–4440.
5 H. Iwata, I. Hirata and Y. Ikada, *Macromolecules*, 1998, **31**, 3671–3678.
6 D. L. Huber, R. P. Manginell, M. A. Samara, B. I. Kim and B. C. Bunker, *Science*, 2003, **301**, 352–354.
7 S. Leibler and D. A. Huse, *J. Cell Biol*., 1993, **121**, 1357–68.
8 R. Yoshida, T. Takahashi, T. Yamaguchi and H. Ichijo, *J. Am. Chem. Soc*., 1996, **118**, 5134–5135.
9 R. Yoshida, E. Kokufuta and T. Yamaguchi, *Chaos*, 1999, **9**, 260–266.
10 R. Yoshida, G. Otoshi, T. Yamaguchi and E. Kokufuta, *J. Phys. Chem. A*, 2001, **105**, 3667–3672.
11 R. Yoshida, T. Sakai, S. Ito and T. Yamaguchi, *J. Am. Chem. Soc*., 2002, **124**, 8095–8098.
12 R. Yoshida, K. Takei and T. Yamaguchi, *Macromolecules*, 2003, **36**, 1759–1761.
13 C. J. Crook, A. Cadby, A. Smith, R. A. L. Jones and A. J. Ryan, *ACS Symp. Ser*,, 2003, **869**, 71–79.
14 C. J. Crook, A. Smith, R. A. L. Jones and A. J. Ryan, *Phys. Chem. Chem. Phys*., 2002, **4**, 1367–1369.
15 R. Iscoff, *Semicond. Int*., 1993, **16**, 58–63.
16 K. Matyjaszewski, P. J. Miller, N. Shukla, B. Immaraporn, A. Gelman, B. B. Luokala, T. M. Siclovan, G. Kickelbick, T. Vallant, H. Hoffmann and T. Pakula, *Macromolecules*, 1999, **32**, 8716–8724.
17 K. L. Beers, S. G. Gaynor, K. Matyjaszewski, S. S. Sheiko and M. Moller, *Macromolecules*, 1998, **31**, 9413–9415.
18 A. Ikker and M. Moller, *New Polym. Mater*., 1993, **4**, 35–51.
19 G. Rabai, M. Orban and I. R. Epstein, *Acc. Chem. Res*., 1990, **23**, 258–63.
20 Y. Tran, P. Auroy and L. T. Lee, *Macromolecules*, 1999, **32**, 8952–8964.
21 H. Yim, M. S. Kent, D. L. Huber, S. Satija, J. Majewski and G. S. Smith, *Macromolecules*, 2003, **36**, 5244–5251; H. Yim, M. S. Kent, S. Mendez, S. S. Balamurugan, S. Balamurugan, G. P. Lopez and S. Satija, *Macromolecules*, 2004, **37**, 1994–1997.
22 W. Bras, I. P. Dolbnya, D. Detollenaere, R. van Tol, M. Malfois, G. N. Greaves, A. J. Ryan and E. Heeley, *J. Appl. Crystallogr*., 2003, **36**, 791–794.
23 J. P. A. Fairclough, C. L. O. Salou, A. J. Ryan, I. W. Hamley, C. Daniel, W. I. Helsby, C. Hall, R. A. Lewis, A. J. Gleeson, G. P. Diakun and G. R. Mant, *Polymer*, 1999, **41**, 2577–2582.
24 E. S. Matsuo and T. Tanaka, *J. Chem. Phys*., 1988, **89**, 1695–703.
25 K. R. Shull, *Mater. Sci. Eng. R*, 2002, **36**, 1–45.
26 D. A. Smith and S. E. Radford, *Curr. Biol.: CB*, 2000, **10**, R662–4.
27 T. Hugel, M. Grosholz, H. Clausen-Schaumann, A. Pfau, H. Gaub and M. Seitz, *Macromolecules*, 2001, **34**, 1039–1047; C. Wang, W. Shi, W. Zhang, X. Zhang, Y. Katsumoto and Y. Ozaki, *Nano Lett*., 2002, **2**, 1169–1172.
28 C. Ortiz and G. Hadziioannou, *Macromolecules*, 1999, **32**, 780–787.
29 A. K. Khandpur, S. Foerster, F. S. Bates, I. W. Hamley, A. J. Ryan, W. Bras, K. Almdal and K. Mortensen, *Macromolecules*, 1995, **28**, 8796–806.
30 J. Yao, P. Ravi, K. C. Tam and L. H. Gan, *Polymer*, 2004, **45**, 2781–2791.